



## Article

# Enzyme Activities in the Lignin Metabolism of Chinese Olive (*Canarium album*) with Different Flesh Characteristics

Jie Wang<sup>1,2</sup> , Jingrong Cai<sup>1,2</sup>, Junyue Zhao<sup>1,2</sup>, Zhixiong Guo<sup>1,2</sup>, Tengfei Pan<sup>1,2</sup>, Yuan Yu<sup>1,2,3,\*</sup> and Wenqin She<sup>1,2,\*</sup>

<sup>1</sup> College of Horticulture, Fujian Agriculture and Forestry University, Fuzhou 350002, China; jiewang202107@163.com (J.W.); jrcai202203@163.com (J.C.); jyzhao202203@163.com (J.Z.); gzhhs@163.com (Z.G.); tfpan@fafu.edu.cn (T.P.)

<sup>2</sup> Institute of Storage, Transportation and Preservation of Horticultural Products, Fujian Agriculture and Forestry University, Fuzhou 350002, China

<sup>3</sup> FAFU-UCR Joint Center for Horticultural Biology and Metabolomics, Haixia Institute of Science and Technology, Fujian Agriculture and Forestry University, Fuzhou 350002, China

\* Correspondence: yyu@fafu.edu.cn (Y.Y.); wenqinshe@fafu.edu.cn (W.S.)

**Abstract:** Lignin is crucial to the formation of fruit texture quality. Here, we aimed to explore the relationship between lignin metabolism and fruit texture by investigating the lignin content, total phenols and their related enzyme activities among three Chinese olive (*Canarium album* (Lour.) Raeusch) genotypes. Our results showed that lignin deposition moved from the exocarp to the flesh in Chinese olive fruit. The lignin, total phenols and enzyme activities were all different between the three Chinese olive cultivars at each developmental stage. The lignin content was positively correlated with the PAL, 4CL and POD activities. These results demonstrated that lignin metabolism was regulated through the related enzyme activities. Therefore, our findings may provide insight to facilitate further improvement in fruit texture quality in Chinese olive.

**Keywords:** *Canarium album*; fruit quality; texture; flavor; phenols



**Citation:** Wang, J.; Cai, J.; Zhao, J.; Guo, Z.; Pan, T.; Yu, Y.; She, W. Enzyme Activities in the Lignin Metabolism of Chinese Olive (*Canarium album*) with Different Flesh Characteristics. *Horticulturae* **2022**, *8*, 408. <https://doi.org/10.3390/horticulturae8050408>

Academic Editor: Daniele Bassi

Received: 27 March 2022

Accepted: 28 April 2022

Published: 6 May 2022

**Publisher's Note:** MDPI stays neutral with regard to jurisdictional claims in published maps and institutional affiliations.



**Copyright:** © 2022 by the authors. Licensee MDPI, Basel, Switzerland. This article is an open access article distributed under the terms and conditions of the Creative Commons Attribution (CC BY) license (<https://creativecommons.org/licenses/by/4.0/>).

## 1. Introduction

Chinese olive (*Canarium album* (Lour.) Raeusch) is an evergreen tree that grows in the tropical and subtropical regions of China. The fruit are rich in various nutrients, such as polyphenols, flavonoids, dietary fiber and calcium. The fresh fruit of Chinese olive is quite popular among customers, as well as their processed fruit. The delicate flesh, crisp texture and few wood fibers make Chinese olive fruit easy to chew and leave a sweet aftertaste. Meanwhile, lignin plays an important role in the fruit texture and quality of Chinese olive [1].

Lignin is crucial to plants, which produces strength and rigidity, delivers water and resists external adverse factors during growth and development [2]. However, more lignin content is not beneficial to fruit. The lignin biosynthetic pathway is widely known (Figure 1). Lignin is an aromatic polymer that is deposited in the secondary cell walls of vascular plants [3]. It derives primarily from the oxidative polymerization of three hydroxycinnamyl alcohol monomers, namely, *p*-coumaryl, coniferyl and sinapyl alcohols, which form the *p*-hydroxyphenyl (H), guaiacyl (G) and syringyl (S) units, respectively [4,5]. In general, lignin is produced mainly through the biosynthesis of lignin monomers and their transportation and polymerization [6]. Lignin biosynthesis is catalyzed via a series of enzymes, including PAL (phenylalanine ammonia-lyase), 4CL (4-coumarate-CoA ligase), CAD (cinnamyl-alcohol dehydrogenase), CCR (cinnamoyl-CoA reductase) and peroxidases (PODs). PAL is the first key rate-limiting enzyme in the metabolic pathway of phenylpropane, catalyzing the deamination of phenylalanine to generate trans-cinnamic acid [7]. Then, 4CL is an upstream key enzyme in the lignin biosynthesis pathway and participates in the production



### 2.2.2. Observation of Lignin Deposition

Lignin deposition was observed with phloroglucinol-hydrochloric acid [12], and the pictures were taken using a Nikon (SMZ25) stereo microscope.

### 2.2.3. Determination of Lignin, Total Phenols Content and Enzyme Activities

The processed sample was taken from the refrigerator at  $-80\text{ }^{\circ}\text{C}$ . Each cultivar and each stage provided three biological replicates, with 63 samples in total. Lignin was extracted with thioglycolic acid and measured spectrophotometrically [13]. The total phenols content was measured according to the method [14,15].

The enzyme activities of PAL, 4CL, CAD and CCR were detected using an enzyme-linked immunosorbent assay kit (Elisa). Briefly, 1 g samples with 10 mL PBS (pH 7.4) were homogenized by hand on ice and centrifuged at  $3000\times g$  ( $4\text{ }^{\circ}\text{C}$ , 20 min). The resultant supernatant was used as the activity assays of PAL, 4CL, CAD and CCR.

POD activity was measured according to the references [16,17]. Briefly, 1 g samples with 5 mL PBS solution (pH 7.0) were grounded on ice, then centrifuged at  $15,000\times g$  ( $4\text{ }^{\circ}\text{C}$ , 15 min) and the supernatant was gathered as an enzyme fluid for testing. The reaction mixture included PBS solution (pH 6.0),  $\text{H}_2\text{O}_2$  (30%) and guaiacol. A total of  $5\text{ }\mu\text{L}$  of enzyme fluid was mixed with a 3 mL reaction mixture for the reactions. A total of  $5\text{ }\mu\text{L}$  of PBS solution (pH 7.0) was used as the reference. The absorbances at 470 nm were determined at 0 min and 5 min, and the difference ( $\Delta\text{A}470$ ) was obtained. The POD active single bit (U) was expressed as the change in absorbance per minute ( $\Delta\text{A}470\cdot\text{min}^{-1}\cdot\text{g}^{-1}$  (FW)).

### 2.2.4. Data Analysis

Excel software was used to analyze the data and make graphs. The analysis of variance (ANOVA) was performed using SPSS software (ver.22.0). Duncan's multiple range test was used to compare the means.

## 3. Results

### 3.1. The Growth and Development Status of Three Chinese Olive Cultivars' Fruit

During the fruit development, the fruit weights of CY, TX and LF first increased and then stayed relatively stable from the 130th DAF (10.42 g) to the 170th DAF (10.34 g) (Figure 2A). The shape index changed slightly during the whole fruit development. The CY fruit was long and spindly (shape index, 1.94), while TX was oval (shape index, 1.51) and LF was elliptical (shape index, 1.73) (Figure 2B).

During fruit development, the CY fruit changed from green to light yellow-green. TX changed from blue-green to green-yellow and LF changed from light green to yellow (Figure 3).

### 3.2. Lignin Deposition in Flesh during Fruit Development

On the 50th DAF, part of the fruit endocarp turned light red and started to become lignified, and the mesocarp presented as light red with a star or dot shape (small part) (Figure 4A). On the 70th DAF, the endocarp was further lignified and appeared dark red. The mesocarp near the endocarp became red with a star or dot shape on the 90th DAF. On the 110th DAF, the color area of the mesocarp spread outward. On the 130th DAF, a large number of woody cells gathered on the vascular bundles of the mesocarp, the endocarp was highly lignified and a hard pit had developed.

The TX fruit was taken as the example to present the crosscutting structure (Figure 4B). The endocarp had a color reaction and lignification on the 50th DAF, and the vascular bundles of the mesocarp appeared pink with a star or dot shape (small part). On the 170th DAF, the endocarp was highly lignified and had a large number of woody cells gathered on the vascular bundles of the mesocarp, which were distributed radially on the mesocarp tissue.

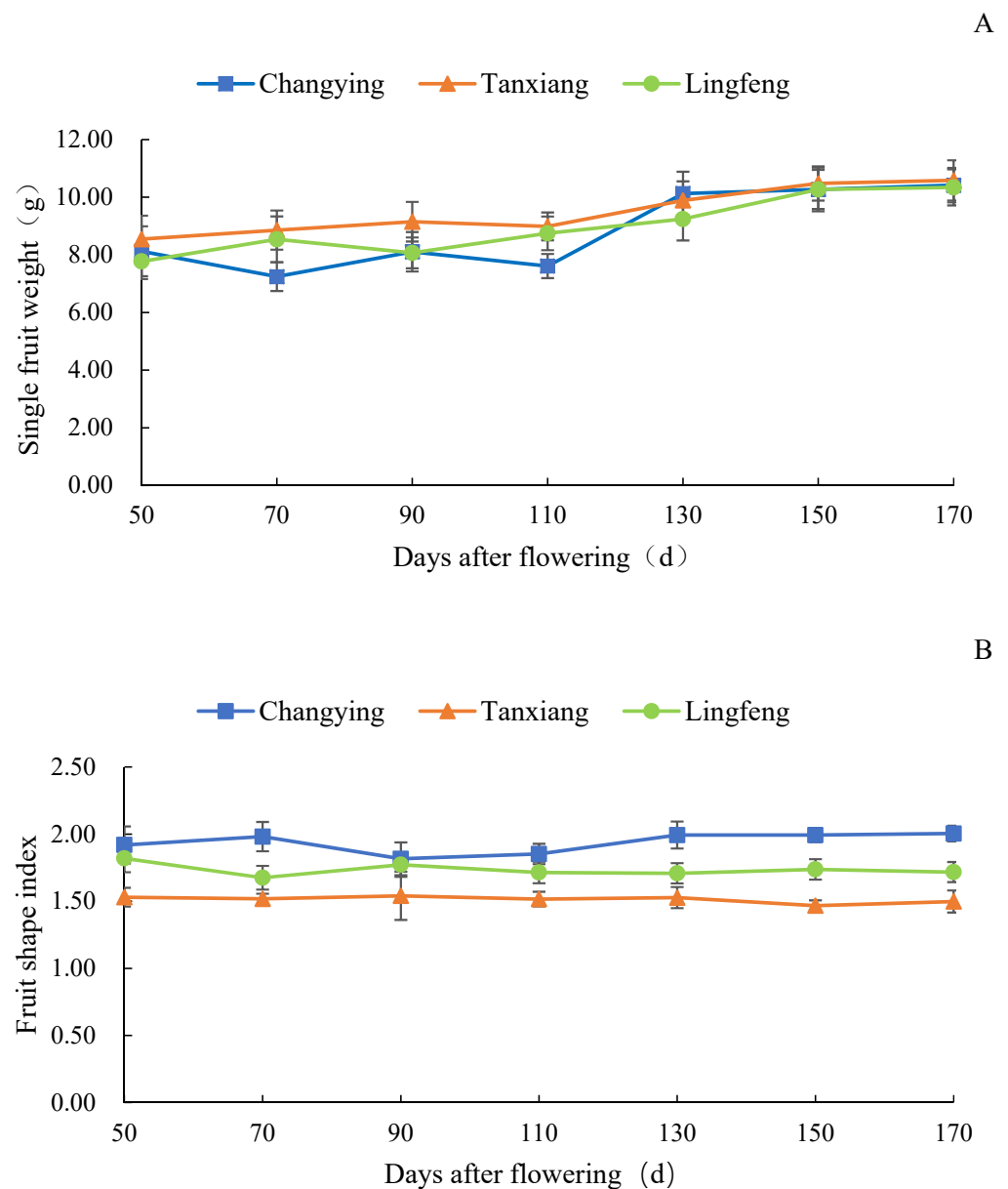


**Figure 2.** Fruit weight and shape indexes of Chinese olives at different developmental stages. (A) Single fruit weight, (B) Fruit shape index.

### 3.3. Lignin Content and Total Phenols in Fruit Flesh at Different Developmental Stages

During fruit development, the changes in lignin differed between the three Chinese olive cultivars (Figure 5A). The lignin content in the CY fruit first increased to the highest value ( $3.73 \text{ mg}\cdot\text{g}^{-1}$ ) on the 70th DAF, decreased later and then rose again from the 90th DAF to the 170th DAF (Figure 5A). The lignin content in TX rose gradually and reached the highest value ( $2.64 \text{ mg}\cdot\text{g}^{-1}$ ) on the 170th DAF (Figure 5A). The lignin in LF rose first and then decreased, the highest value of lignin content ( $2.87 \text{ mg}\cdot\text{g}^{-1}$ ) appeared on the 130th DAF and then dropped sharply to the final stage (Figure 5A). On the 170th DAF, the LF fruit contained a lower amount of lignin than the other two cultivars (Figure 5A).

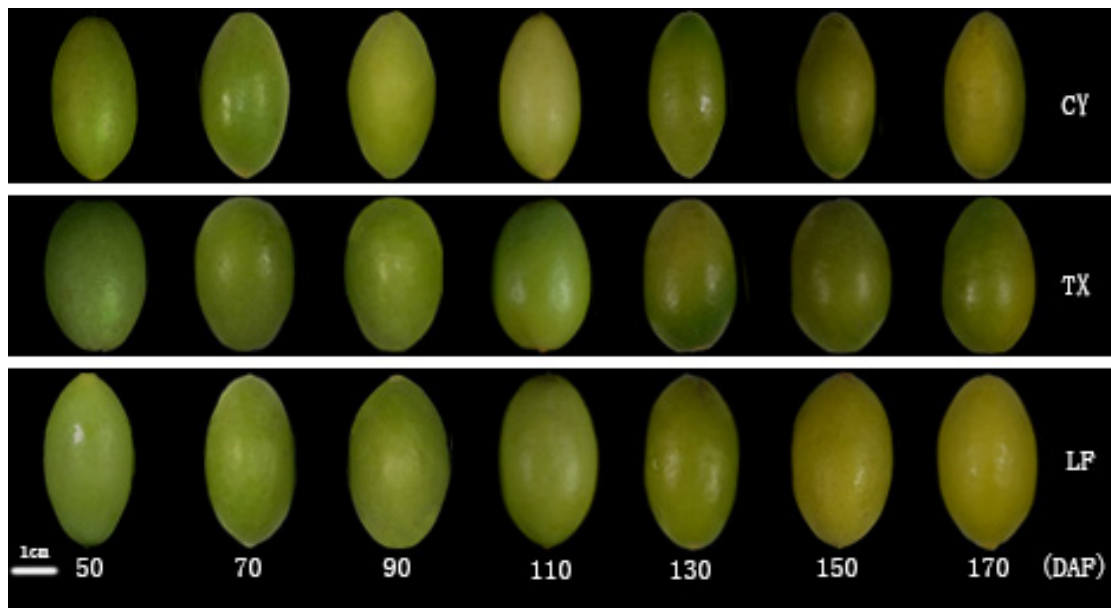


**Figure 3.** Chinese olive fruit at different developmental stages. CY, ‘Changying’, TX, ‘Tanxiang’, LF, ‘Lingfeng’. DAF, days after flowering.

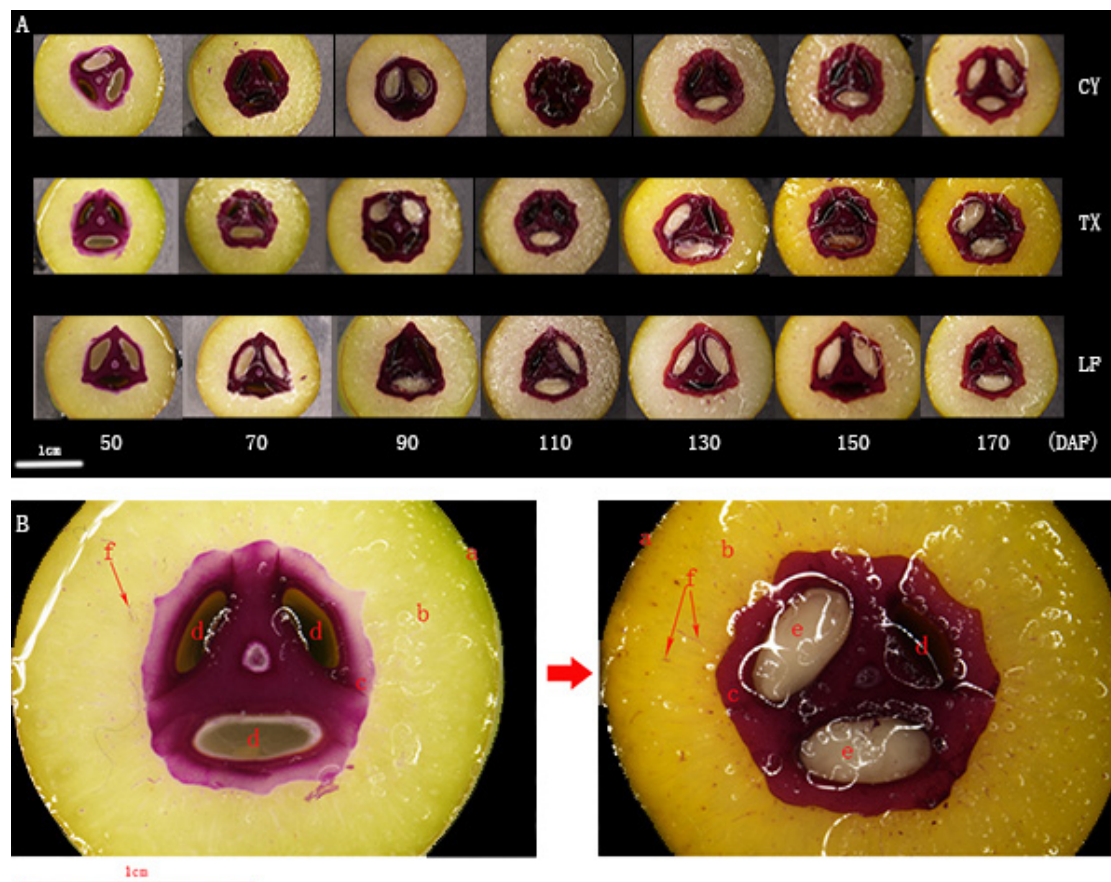


**Figure 4.** Lignin staining in fruit flesh of Chinese olive at different developmental stages. (A) CY, ‘Changying’, TX, ‘Tanxiang’, LF, ‘Lingfeng’. DAF, days after flowering. (B) a, exocarp; b, mesocarp; c, endocarp (color reaction of phloroglucinol-hydrochloric acid); d, seed room; e, seed; f, vascular bundle (color reaction of phloroglucinol-hydrochloric acid). The left image: 50 DAF (the stage of fruit pulp filling and core hardening), and the right image: 170 DAF (the stage of fruit maturity).

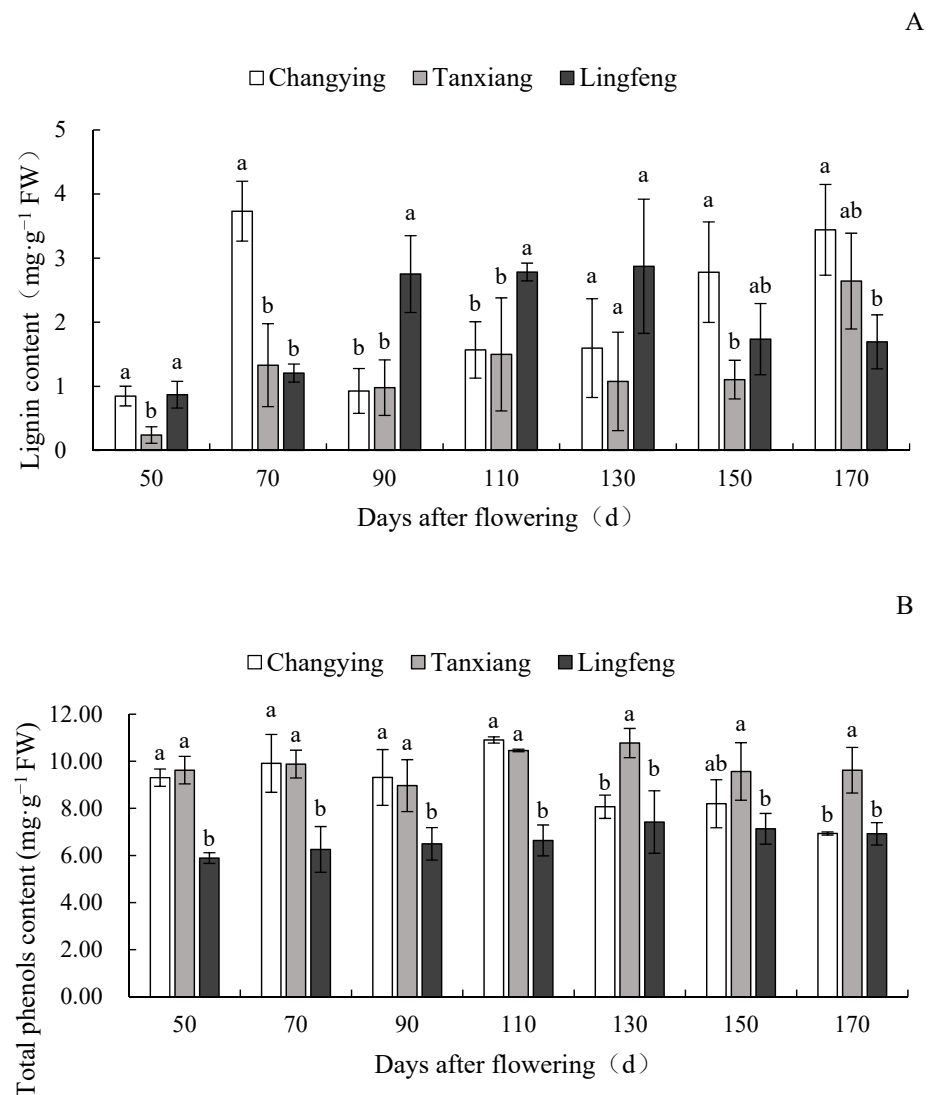


**Figure 5.** Concentrations of lignin and total phenols among three Chinese olive cultivars at different fruit developmental stages. Different letters indicate significant differences between different varieties within each stage ( $p < 0.05$ ). (A) Lignin, (B) Total phenols.

The trend of change in total phenols content first rose and then dropped in all three Chinese olive cultivars (Figure 5B). The total phenols in the CY fruit changed greatly during the whole process, while that in TX and LF changed slightly (Figure 5B). The total phenols in CY fruit rose sharply, up to the highest value ( $10.91 \text{ mg}\cdot\text{g}^{-1}$ ) on the 110th DAF, while the highest values of total phenols in TX ( $10.71 \text{ mg}\cdot\text{g}^{-1}$ ) and LF ( $7.42 \text{ mg}\cdot\text{g}^{-1}$ ) both appeared on the 130th DAF (Figure 5B). In general, the total phenols in CY and TX were higher than that in LF during the fruit development (Figure 5B).

### 3.4. Measurement of the Activities of Lignin-Metabolism-Related Enzymes

During fruit development, the PAL activities presented an M-shaped trend in all three Chinese olive cultivars and maintained a low level on the 50th DAF (Figure 6A). The PAL activities in the CY and TX fruit were the highest on the 150th DAF, which was 20 days later than that in LF (Figure 6A). On the 170th DAF, the PAL activities dropped in all three Chinese olive cultivars (Figure 6A).

However, the 4CL activities changed differently between the three Chinese olive cultivars (Figure 6B). The 4CL activity in CY fruit first dropped, rose later, then dropped and rose again, which reached the highest value on the 90th DAF (Figure 6B). The 4CL

activity in TX first rose and then dropped, and the highest value appeared on the 150th DAF (Figure 6B). The 4CL activity in LF first went up, fell later, then rose and declined again, and the highest value appeared on the 130th DAF (Figure 6B). In general, the 4CL activities changed significantly in all the three Chinese olive cultivars from the 90th to 130th DAF (Figure 6B). On the 170th DAF, the 4CL activity in TX was significantly lower than that in CY and LF (Figure 6B).

The CAD activities first rose and then declined in all three Chinese olive fruit (Figure 6C). The highest values of CAD activity in CY, TX and LF appeared on the 110th DAF, 90th DAF and 130th DAF, respectively (Figure 6C). The CAD activities changed greatly from the 70th to 110th DAF in all three cultivars (Figure 6C). From the 150th to 170th DAF, the CAD activity in LF was obviously lower than that in the other two (Figure 6C).

The CCR activities changed differently from each other among the three cultivars (Figure 6D). The CCR activity in CY first dropped and then increased to the highest value on the 170th DAF, while CCR activities in TX and LF first rose and then dropped (Figure 6D). The CCR activities in TX and LF reached the highest value on the 130th DAF and 70th DAF, respectively (Figure 6D). On the 170th DAF, the CCR activity in CY was obviously higher than that in the other two (Figure 6D).

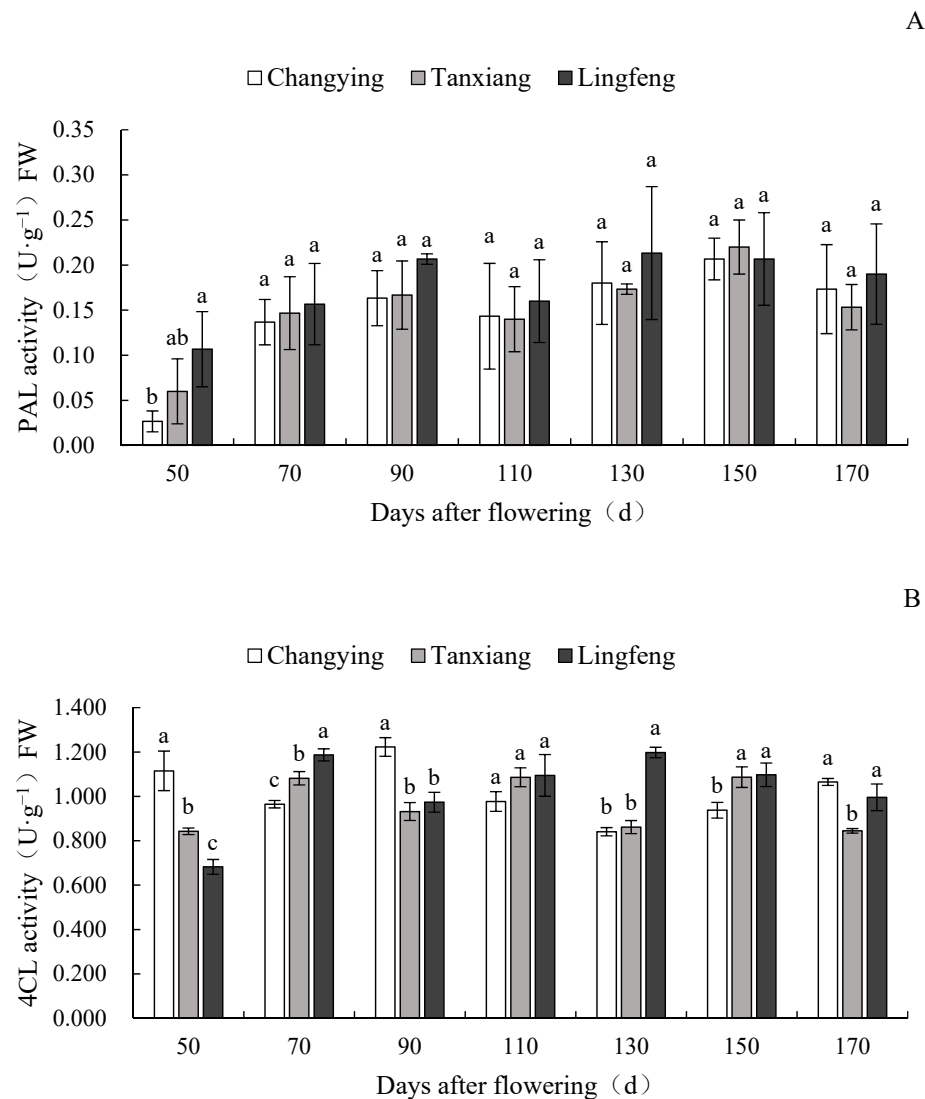
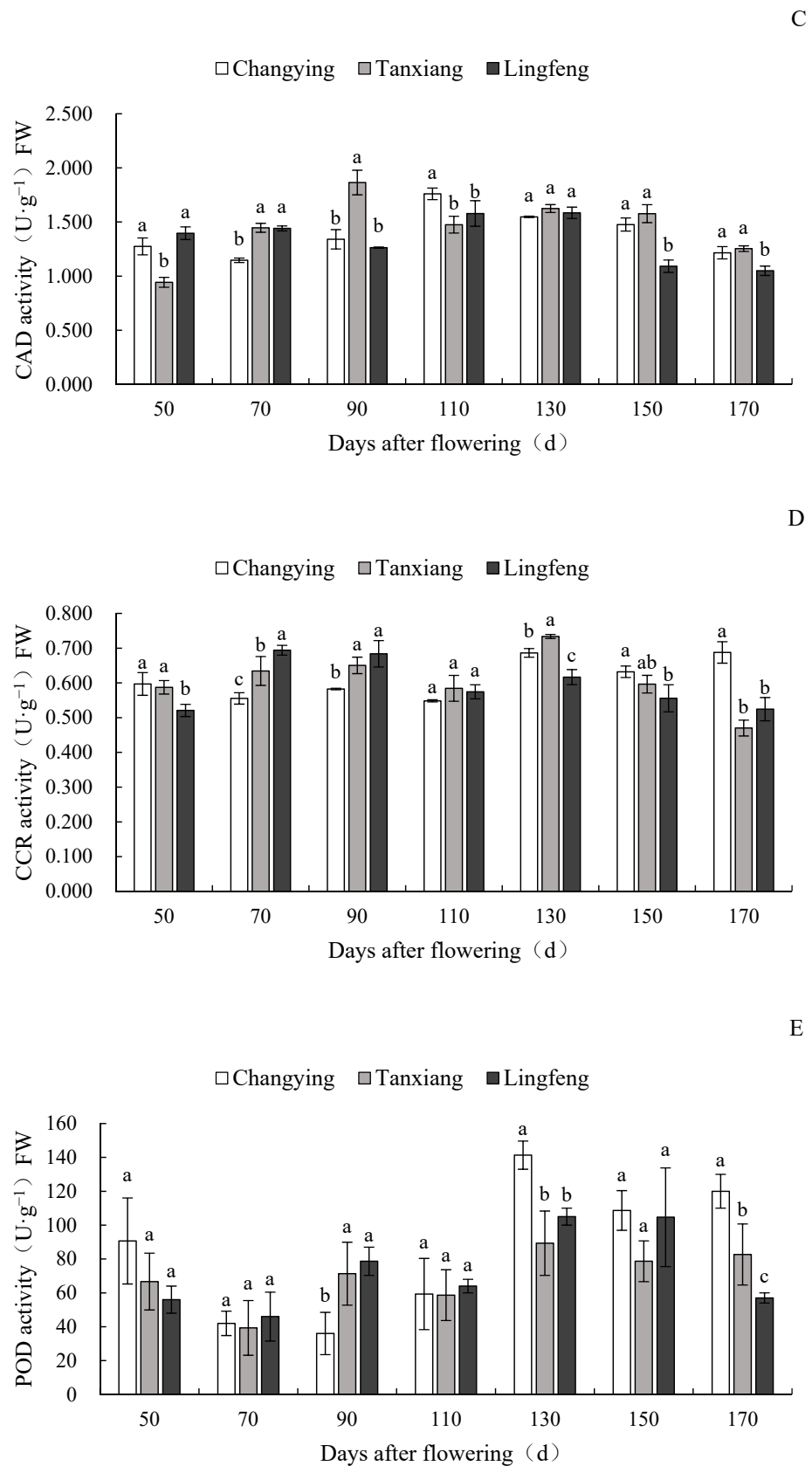


Figure 6. Cont.



**Figure 6.** Activities of lignin synthesis enzymes in Chinese olive fruit at different developmental stages. Different letters indicate significant differences between the three varieties within each stage ( $p < 0.05$ ). (A) PAL, (B) 4CL, (C) CAD, (D) CCR and (E) POD.



The POD activities first declined, rose later and then declined again in all three cultivars (Figure 6E). On the 170th DAF, the POD activity in CY was obviously higher than that in TX and LF (Figure 6E).

### 3.5. Correlation Analysis

There was a negative correlation between lignin content and total phenols (Table 1). In contrast, lignin content was positively correlated with PAL, 4CL and POD enzyme activities but negatively correlated with CAD and CCR enzyme activities (Table 1). Furthermore, total phenols were positively correlated with CAD enzyme activities but negatively correlated with PAL, 4CL, CCR and POD enzyme activities (Table 1).

**Table 1.** Correlation analysis of lignin content, total phenol and enzyme activities.

	Lignin Content	Total Phenols	PAL	4CL	CAD	CCR	POD
Lignin Content	1	−0.252	0.426	0.119	−0.110	−0.025	0.264
Total Phenols		1	−0.289	−0.049	0.218	−0.080	−0.195
PAL			1	0.208	0.258	0.238	0.286
4CL				1	0.042	0.143	−0.158
CAD					1	0.323	0.062
CCR						1	0.353
POD							1

## 4. Discussion

Chinese olive is a kind of stone fruit, and the flesh is made up of an exocarp and mesocarp. The exocarp consists of an epidermal cell layer, while the mesocarp is regularly scattered with vascular bundles, and the endocarp develops into a hard pit. In this study, we found that lignin deposition in Chinese olive fruit first started from the exocarp and spread outward; then, the vascular tissue of the flesh was gradually lignified. During the maturing stage, the endocarp was highly lignified, and the vascular bundles of the mesocarp presented lignin distribution in the three Chinese olive cultivars.

Lignin metabolism in plants was widely reported. For example, lignin content increased initially and decreased afterward during pear fruit development [18]. In tobacco leaves, the accumulation of lignin gradually increased first, then slowly decreased during maturation [19]. Here, we discovered that the changes in lignin content differed between the three Chinese olive cultivars, and may have caused the diverse range of fruit textures.

Lignin and its precursors, namely, phenols, are both derived from the phenylpropane metabolic pathway. In fresh waxy corn, the lignin content was significantly correlated with the polyphenol content and firmness [20]. The fruit firmness and lignin content increased while the total phenols decreased in damaged mangosteen pericarp [21]. Interestingly, the increase in the firmness of mangosteen pericarp after impact was related to the increased activities of the enzymes required for lignin biosynthesis but not for phenol biosynthesis [22]. In this work, the total phenols content changed differently between the three cultivars during the whole developmental process. Correlation analysis showed that total phenols content was negatively correlated with lignin content, suggesting that total phenols were related to lignin biosynthesis.

Lignin biosynthesis involves a series of enzymes, including PAL, 4CL, CAD, CCR and POD [23]. The lignin content is closely related to the enzyme activities of PAL, 4CL, CAD and POD in buckwheat [24]. It was reported that PAL, CAD and POD are involved in lignin biosynthesis in postharvest bamboo shoots [25], and similar results were also found in loquat [26] and mangosteen [27]. The accumulation of lignin in the flesh tissue of water bamboo shoots was positively correlated with PAL and POD activities [28]. The rise in PAL activity did not necessarily result in an increase in lignin in cherimoya fruit [29].

Furthermore, 4CL was suggested to participate in the regulation of lignin and flavonoid biosynthesis in Chinese pear [30]. POD activity was related to lignin content in *Arabidopsis thaliana* [31]. Here, PAL activities generally presented an M-shaped trend during the process of ripening and showed no significant differences between the three Chinese olive cultivars within each stage from the 70th DAF to 170th DAF. The M-shaped trend indicated that PAL activities produced two peaks. The first peak may signify the growth of fruit, while the second peak showed the rapid synthesis of substance-influenced fruit flavor. The 4CL activities were significantly different between the three Chinese olive cultivars within each stage from the 50th DAF to 90th DAF and from the 130th DAF to 170th DAF. Moreover, CAD, CCR and POD are the key downstream enzymes for lignin biosynthesis. Herein, we discovered that CAD and CCR activities changed differently between the three cultivars during fruit development. POD activities in all three cultivars declined in the early stage and then rose in the middle and late stages during fruit development. Correlation analysis found that the PAL, 4CL and POD activities were positively correlated with lignin content, indicating that they may be involved in lignin biosynthesis. On the other side, CAD and CCR activities were negatively correlated with lignin content, which revealed that they may not be the key enzymes for lignin biosynthesis and are involved in upstream reactions.

## 5. Conclusions

In the present study, we explored the formation of fruit texture and quality in Chinese olive with different flesh characteristics via the lignin metabolism pathway. We found that lignin metabolism was involved in the development of fruit texture and quality. The lignin content and PAL, 4CL and POD enzyme activities were the important factors for developing different fruit textures. In further study, we will explore the molecular mechanisms for lignin formation to improve the fruit quality and flavor of Chinese olives.

**Author Contributions:** J.W.: investigation, resources, writing—original draft and software. J.C. and J.Z.: investigation and resources. Z.G.: conceptualization, methodology and data curation. T.P.: project administration and validation. Y.Y.: writing—review and editing and supervision. W.S.: supervision and funding acquisition. All authors have read and agreed to the published version of the manuscript.

**Funding:** This research was funded by [the National Finance Forestry Science and Technology Promotion Project of China] grant number [363, 2021-2023]. And The APC was funded by [the Community of Fujian Famous and Quality Fruit Tree in Industrial Service].

**Institutional Review Board Statement:** Not applicable.

**Informed Consent Statement:** Not applicable.

**Data Availability Statement:** Not applicable.

**Conflicts of Interest:** The authors declare no conflict of interest.

## Abbreviations

PAL, phenylalanine ammonia-lyase; 4CL, 4-coumarate–CoA ligase; CAD, cinnamyl-alcohol dehydrogenase; CCR, cinnamoyl-CoA reductase; POD, peroxidase; FW, fresh weight; DAF, days after flowering. CY, Changying, TX, Tanxiang, LF, Linfeng; Raesch, Ernst Adolf Raeschel.

## References

1. Lu, G.; Li, Z.; Zhang, X.; Wang, R.; Yang, S. Expression Analysis of Lignin-Associated Genes in Hard End Pear (*Pyrus pyrifolia* Whangkeumbae) and Its Response to Calcium Chloride Treatment Conditions. *J. Plant Growth Regul.* **2015**, *34*, 251–262. [[CrossRef](#)]
2. Peter, G.; Neale, D. Molecular basis for the evolution of xylem lignification. *Curr. Opin. Plant Biol.* **2004**, *7*, 737–742. [[CrossRef](#)] [[PubMed](#)]
3. Vanholme, R.; Demedts, B.; Morreel, K.; Ralph, J.; Boerjan, W. Lignin Biosynthesis and Structure. *Plant Physiol.* **2010**, *153*, 895–905. [[CrossRef](#)]
4. Boerjan, W.; Ralph, J.; Baucher, M. Lignin Biosynthesis. *Annu. Rev. Plant Biol.* **2003**, *54*, 519–546. [[CrossRef](#)] [[PubMed](#)]

5. Sattler, S.E.; Funnell-Harris, D.L. Modifying lignin to improve bioenergy feedstocks: Strengthening the barrier against pathogens? *Front. Plant Sci.* **2013**, *4*, 70. [[CrossRef](#)] [[PubMed](#)]
6. Liu, Q.Q.; Luo, L.; Zheng, L.Q. Lignins: Biosynthesis and Biological Functions in Plants. *Int. J. Mol. Sci.* **2018**, *19*, 335. [[CrossRef](#)]
7. MacDonald, M.J.; D’Cunha, G.B. A modern view of phenylalanine ammonia lyase. *Biochem. Cell Biol.* **2007**, *85*, 759. [[CrossRef](#)]
8. Sutela, S.; Hahl, T.; Tiimonen, H.; Aronen, T.; Ylioja, T.; Laakso, T.; Saranpaa, P.; Chiang, V.; Julkunen-Tiitto, R.; Haggman, H. Phenolic Compounds and Expression of 4CL Genes in Silver Birch Clones and Pt4CL1a Lines. *PLoS ONE* **2014**, *9*, e114434. [[CrossRef](#)]
9. Tao, S.T.; Khanizadeh, S.; Zhang, H.; Zhang, S.L. Anatomy, ultrastructure and lignin distribution of stone cells in two *Pyrus species*. *Plant Sci.* **2009**, *176*, 413–419. [[CrossRef](#)]
10. Su, X.; Zhao, Y.; Wang, H.; Li, G.; Cheng, X.; Jin, Q.; Cai, Y. Transcriptomic analysis of early fruit development in Chinese white pear (*Pyrus bretschneideri* Rehd.) and functional identification of PbCCR1 in lignin biosynthesis. *BMC Plant Biol.* **2019**, *19*, 417. [[CrossRef](#)]
11. Fagerstedt, K.V.; Kukkola, E.M.; Koistinen, V.V.T.; Takahashi, J.; Marjamaa, K. Cell Wall Lignin is Polymerised by Class III Secretable Plant Peroxidases in Norway Spruce. *J. Integr. Plant Biol.* **2010**, *52*, 186–194. [[CrossRef](#)] [[PubMed](#)]
12. Zhang, X.; Zhang, L.J.; Zhang, Q.P.; Xu, J.Y.; Liu, W.S.; Dong, W.X. Comparative transcriptome profiling and morphology provide insights into endocarp cleaving of apricot cultivar (*Prunus armeniaca* L.). *BMC Plant Biol.* **2017**, *17*, 72. [[CrossRef](#)] [[PubMed](#)]
13. Wang, G.L.; Huang, Y.; Zhang, X.Y.; Xu, Z.S.; Wang, F.; Xiong, A.S. Transcriptome-based identification of genes revealed differential expression profiles and lignin accumulation during root development in cultivated and wild carrots. *Plant Cell Rep.* **2016**, *35*, 1743–1755. [[CrossRef](#)] [[PubMed](#)]
14. Reichel, M.; Carle, R.; Sruamsiri, P.; Neidhart, S. Changes in flavonoids and nonphenolic pigments during on-tree maturation and postharvest pericarp browning of litchi (*Litchi chinensis* Sonn.) as shown by HPLC-MSn. *J. Agric. Food Chem.* **2011**, *59*, 3924–3939. [[CrossRef](#)] [[PubMed](#)]
15. Lin, Y.; Chen, Q.; Guan, X.; Chen, M.; Ou, G. Extraction of Total Polyphenol from Chinese Olive (*Canarium ablum* L.). *Chin. Agric. Sci. Bull.* **2011**, *27*, 396–400. (In Chinese)
16. Maehly, A.C.; Chance, B. The assay of catalases and peroxidases. *Methods Biochem. Anal.* **1954**, *1*, 357–424. [[CrossRef](#)]
17. Pan, T.; Zhu, X.; Pan, D.; Guo, Z.; She, W.; Chen, G. Relationship between granulation and lignin metabolism in ‘Guanximiyou’ pummelo fruit during storage. *J. Fruit Sci.* **2013**, *30*, 294–298. (In Chinese) [[CrossRef](#)]
18. Cai, Y.P.; Li, G.Q.; Nie, J.Q.; Lin, Y.; Nie, F.; Zhang, J.Y.; Xu, Y.L. Study of the structure and biosynthetic pathway of lignin in stone cells of pear. *Sci. Hortic.* **2010**, *125*, 374–379. [[CrossRef](#)]
19. Song, Z.P.; Wang, D.B.; Gao, Y.B.; Li, C.J.; Jiang, H.L.; Zhu, X.W.; Zhang, H.Y. Changes of lignin biosynthesis in tobacco leaves during maturation. *Funct. Plant Biol.* **2021**, *48*, 624–633. [[CrossRef](#)]
20. Gong, K.J.; Chen, L.R.; Li, X.Y.; Liu, K.C. Lignin accumulation and biosynthetic enzyme activities in relation to postharvest firmness of fresh waxy corn. *J. Food Processing Preserv.* **2018**, *42*, e13333. [[CrossRef](#)]
21. Bunsiri, A.; Ketsa, S.; Paull, R.E. Phenolic metabolism and lignin synthesis in damaged pericarp of mangosteen fruit after impact. *Postharvest Biol. Technol.* **2003**, *29*, 61–71. [[CrossRef](#)]
22. Bunsiri, A.; Paull, R.E.; Ketsa, S. Increased activities of phenylalanine ammonia lyase, peroxidase, and cinnamyl alcohol dehydrogenase in relation to pericarp hardening after physical impact in mangosteen (*Garcinia mangostana* L.). *J. Hortic. Sci. Biotechnol.* **2012**, *87*, 231–236. [[CrossRef](#)]
23. Vanholme, R.; Storme, V.; Vanholme, B.; Sundin, L.; Christensen, J.H.; Goeminne, G.; Halpin, C.; Rohde, A.; Morreel, K.; Boerjan, W. A Systems Biology View of Responses to Lignin Biosynthesis Perturbations in Arabidopsis. *Plant Cell* **2012**, *24*, 3506–3529. [[CrossRef](#)] [[PubMed](#)]
24. Hu, D.; Liu, X.B.; She, H.Z.; Gao, Z.; Ruan, R.W.; Wu, D.Q.; Yi, Z.L. The lignin synthesis related genes and lodging resistance of *Fagopyrum esculentum*. *Biol. Plant.* **2017**, *61*, 138–146. [[CrossRef](#)]
25. Luo, Z.S.; Feng, S.M.; Pang, J.; Mao, L.C.; Shou, H.L.; Xie, J.W. Effect of heat treatment on lignification of postharvest bamboo shoots (*Phyllostachys praecox* f. *prevernalis*). *Food Chem.* **2012**, *135*, 2182–2187. [[CrossRef](#)]
26. Cai, C.; Xu, C.J.; Li, X.; Ferguson, I.; Chen, K.S. Accumulation of lignin in relation to change in activities of lignification enzymes in loquat fruit flesh after harvest. *Postharvest Biol. Technol.* **2006**, *40*, 163–169. [[CrossRef](#)]
27. Dangcham, S.; Bowen, J.; Ferguson, I.B.; Ketsa, S. Effect of temperature and low oxygen on pericarp hardening of mangosteen fruit stored at low temperature. *Postharvest Biol. Technol.* **2008**, *50*, 37–44. [[CrossRef](#)]
28. Miao, M.; Wang, Q.X.; Zhang, T.; Jiang, B. Effect of high hydrostatic pressure (HHP) treatment on texture changes of water bamboo shoots cultivated in China. *Postharvest Biol. Technol.* **2011**, *59*, 327–329. [[CrossRef](#)]
29. Assis, J.S.; Maldonado, R.; Muñoz, T.; Escribano, M.I.; Merodio, C. Effect of high carbon dioxide concentration on PAL activity and phenolic contents in ripening cherimoya fruit. *Postharvest Biol. Technol.* **2001**, *23*, 33–39. [[CrossRef](#)]
30. Cao, Y.; Han, Y.; Li, D.; Lin, Y.; Cai, Y. Systematic Analysis of the 4-Coumarate:Coenzyme A Ligase (4CL) Related Genes and Expression Profiling during Fruit Development in the Chinese Pear. *Genes* **2016**, *7*, 89. [[CrossRef](#)]
31. Cosio, C.; Dunand, C. Transcriptome analysis of various flower and silique development stages indicates a set of class III peroxidase genes potentially involved in pod shattering in *Arabidopsis thaliana*. *BMC Genom.* **2010**, *11*, 528. [[CrossRef](#)] [[PubMed](#)]